Time-Optimal Motions of Robots in Assembly Tasks

HANS P. GEERING, SENIOR MEMBER, IEEE, LINO GUZZELLA, STEPHAN A. R. HEPNER, AND CHRISTOPHER H. ONDER

Abstract—**For a cylindrical, and a spherical robot, and a robot with a horizontal articulated arm with two links, time-optimal unconstrained trajectories for arbitrary fixed initial and final positions are calculated. The exact equations of motion are utilized. The controls (torques and forces) are limited. The general structure of the optimal solution is discussed and explained physically for each robot. The importance of such analyses during the mechanical design of a robot is pointed out. The reduction of the duration of an optimal motion, compared to more straightforward and natural ones, and hence the increase of the productivity of the robot in an assembly cycle can be considerable. The numerical examples include the "Automelec ACR" and the "IBM 7535 B 04" robots.**

I. Introduction

A ROBOT performing an automated assembly task repeatedly goes through the following generic sequence of steps: 1) move to the location where a component (or subassembly) is stacked; 2) grasp the component; 3) transport it to the location of assembly; and 4) mount it onto the partially finished product. In order to maximize the productivity of the robot, the total assembly time must be minimized, i.e., both the layout of the components' stacks around the workpiece must be optimized and each of the steps of assembly must be executed in minimal time. In this paper, only the problem of finding time-optimal motions for the various (prespecified) steps 1) and 3) is addressed.

The problem of time-optimal motions was first treated in [1]. In this thesis, several regular time-optimal trajectories for a hydraulic robot with an articulated arm and three degrees of freedom were calculated. The major portion of this work consisted of finding a closed-loop regulation around the time-optimal nominal trajectory using linearization, gravity compensation, and averaged compensation of the effects of angular speeds. The possibility of singular time-optimal control was not investigated.

About ten years later, the interest in time-optimality of robot motions increased significantly [2], [4]–[6], [8]. In [6], the optimization problem was stated completely and the available mathematical design tools were discussed. In [2], a recursive scheme converging to the time-optimal solution was presented and applied to a trainable manipulator with seven degrees of freedom. A similar, adaptive scheme for a two-link robot was given in [4]. In [5], an approximately time-optimal controller was combined with a linear regulator for the final phase of the trajectory. The dynamic programming method of synthesis of optimal trajectories was treated in [8]. This paper addressed energy-optimal control but the method is directly applicable to time optimality as discussed in [6]. Since the complexity of the necessary calculations for time-optimal control is considerable, several schemes for simplification were proposed. The problem of time-optimal motion along arbitrary prespecified spatial trajectories was studied in [10], [11], and [13]. The special case of rectilinear motion was published in [7]. In this method there is only one degree of freedom, viz. the acceleration along the trajectory. The problem of specifying this trajectory remains. The method of parameter optimization was used in [9]. It reduces the optimal control problem to the problem of finding a suitable parametrization for the control variables. In [3], open-loop and closed-loop suboptimal solutions were found by solving algebraic equations.

Apparently, the complete (structure of the) solution to the problem of time-optimal motion of a robot with more than one degree of freedom has never been published. In particular, the question of existence of time-optimal controls containing singular arcs (where the control variables are not necessarily bang-bang) is open.

The purpose of this paper is to discuss the structure of the time-optimal control for arbitrary point-to-point transfers for three rather common robot geometries. The cylindrical robot, the spherical robot, and a horizontal articulated arm with two degrees of freedom are investigated in Sections II, III, and IV, respectively. Section V contains some remarks about the mathematical tools used in the analysis. In the concluding Section VI, the philosophy behind this piece of research is discussed and some open research problems are mentioned.

II. Robot with Cylindrical Coordinates

In this section, the time-optimal control problem for a cylindrical robot with two degrees of freedom is investigated in some detail. The equations of motion are given in Section II-A and the optimal control problem is stated in Section II-B. The relevant parts of the analysis of the problem are contained in Section II-C. In Section II-D, the structure of the complete optimal solution is described and explained.

A. The Model

The geometry of the cylindrical robot is depicted in Fig. 1. In the general case, the first degree of freedom is the vertical translation z. This coordinate is not treated here because it is completely decoupled both from the second and the third coordinate and because the Automelec ACR robot does not have it. The second degree of freedom is the azimuth rotation φ. This coordinate is driven by a limited torque M. The third degree of freedom is the radial translation r (measured between the azimuth axis and the center of gravity S of the naked arm which has mass m_a). It is driven by a limited force F. The remaining degrees of freedom are in the robot's hand. Their influence is neglected and the hand and the load are lumped into a point mass m_n.

With the state variables

$$x_1(t) = r(t) \tag{1}$$

$$x_2(t) = \dot{r}(t) \tag{2}$$

$$x_3(t) = \varphi(t) \tag{3}$$

$$x_4(t) = \dot{\varphi}(t) \tag{4}$$

Manuscript received March 21, 1985; revised September 16, 1985. Paper recommended by Associate Editor, W. J. Book. This work was supported in part by Schweizerischer Schulrat under Grant 330.083.11/4.

The authors are with The Swiss Federal Institute of Technology (ETH), Zurich, Switzerland.

IEEE Log Number 8608338.

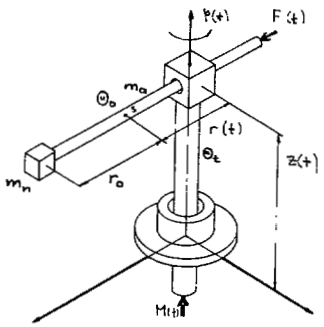

Fig. 1. Sketch of the cylindrical robot.

and the control variables

$$u_1(t) = F(t) \tag{5}$$

$$u_2(t) = M(t) \tag{6}$$

and neglecting friction the equations of motion are

$$\dot{x}_1(t) = x_2(t) \tag{7}$$

$$\dot{x}_2(t) = [u_1(t) + m_a x_1(t) x_4^2(t) + m_n \{r_0 + x_1(t)\} x_4^2(t)]/(m_a + m_n) \tag{8}$$

$$\dot{x}_3(t) = x_4(t) \tag{9}$$

$$\dot{x}_4(t) = [u_2(t) - 2m_a x_1(t) x_2(t) x_4(t) - 2m_n \{r_0 + x_1(t)\} x_2(t) x_4(t)]/\theta_{\text{tot}}(x_1(t)) \tag{10}$$

where

$$\theta_{\text{tot}}(x_1(t)) = \theta_t + \theta_0 + m_a x_1^2(t) + m_n \{r_0 + x_1(t)\}^2 \tag{11}$$

and θ_t is the mass moment of inertia of the robot without the arm, hand, and load (w.r. to the azimuth axis), θ_0 is the mass moment of inertia of the naked robot arm without the load (w.r. to its center of gravity S), and r_0 is the distance between the lumped mass m_n and S.

The control constraints are

$$|u_1(t)| \le F_{\max} \tag{12}$$

$$|u_2(t)| \le M_{\max}. \tag{13}$$

For the numerical calculations the following values were used for the Automelec ACR robot:

$$m_a = 3.7 \text{ kg} \quad m_n = 4.6 \text{ kg} \quad r_0 = 0.37 \text{ m}$$

$$\theta_t = 0.28 \text{ m}^2\text{kg} \quad \theta_0 = 0.09 \text{ m}^2\text{kg}$$

$$F_{\max} = 15 \text{ N} \quad M_{\max} = 5 \text{ Nm}. \tag{14}$$

B. The Optimal Control Problem

For the assembly robot, time-optimal motions from an arbitrary initial position (at standstill)

$$x_1(0) = r_a \tag{15}$$

$$x_3(0) = \varphi_a \tag{16}$$

$$x_2(0) = x_4(0) = 0 \tag{17}$$

to an arbitrary final position (at standstill)

$$x_1(T) = r_b \tag{18}$$

$$x_3(T) = \varphi_b \tag{19}$$

$$x_2(T) = x_4(T) = 0 \tag{20}$$

are to be found.

The complete statement of the optimal control problem is as follows.

For the robot governed by the differential equations (7)–(11) find admissible controls u_1 and u_2 satisfying the constraints (12) and (13) which transfer the robot from the fixed initial state (15)–(17) to the fixed final state (18)–(20) such that the cost functional

$$J(u) = \int_0^T dt \tag{21}$$

is minimized.

Notice that no state constraints have been included in the statement of the optimal control problem. The philosophy here is the following. When the mechanical design of a new robot is done, the complete structure of the time-optimal motion (for arbitrary initial and final positions) without state constraints should be known. This knowledge should be used when the (unavoidable) state constraints have to be specified. Similarly, it should be used in the mechanical design (masses, inertias) and in the choice of the control constraints.

C. Analysis of the Optimal Control Problem

For the analysis of the optimal control problem, Pontryagin's minimum principle [12] is used. With the costate variables $p_1(t)$, $p_2(t)$, $p_3(t)$, and $p_4(t)$, and the nonnegative constant $p_0 (= 0 \text{ or } 1)$ the Hamiltonian function is

$$H = p_0 + p_1(t)\dot{x}_1(t) + p_2(t)\dot{x}_2(t) + p_3(t)\dot{x}_3(t) + p_4(t)\dot{x}_4(t). \tag{22}$$

It is affine in the controls, i.e., it is of the form

$$H = f(x, p) + h_1(x, p)u_1 + h_2(x, p)u_2 \tag{23}$$

where

$$h_1(x, p) = p_2(t)/(m_a + m_n) \tag{24}$$

and

$$h_2(x, p) = p_4(t)/\theta_{\text{tot}}(x_1(t)) \tag{25}$$

are the switching functions, and $f(x, p)$ collects the remaining terms defined by (22) and (7)–(11).

The costate variables satisfy the linear adjoint differential equations

$$\dot{p}_i(t) = -\partial H/\partial x_i \qquad \text{for } i = 1 \cdots 4. \tag{26}$$

Their boundary values at $t = 0$ and $t = T$ are free because the initial and final states are fixed. Furthermore, since the final time T is free and the problem is time-invariant, the Hamiltonian vanishes along the optimal trajectory

$$H \equiv 0. \tag{27}$$

The optimal controls are obtained by globally minimizing the Hamiltonian with respect to u_1 and u_2. Hence, the optimal controls are essentially determined by the signs of the switching functions h_1 and h_2. Since both of the denominators in (24) and (25) are positive, the signs of $p_2(t)$ and $p_4(t)$ are relevant, respectively. More precisely, the optimal control laws are

$$u_1(t) = +F_{\max} \qquad \text{for } p_2(t) < 0$$

$$u_1(t) = -F_{\max} \qquad \text{for } p_2(t) > 0$$

$$u_1(t) = \text{arbitrary for } p_2(t) = 0 \text{ at isolated times only}$$

$u_1(t)$ is singular for $p_2(t) \equiv 0$ in a subinterval of $[0, T]$ (28)

and

$$u_2(t) = +M_{\max} \quad \text{for } p_4(t) < 0$$

$$u_2(t) = -M_{\max} \quad \text{for } p_4(t) > 0$$

$$u_2(t) = \text{arbitrary for } p_4(t) = 0 \text{ at isolated times only}$$

$u_2(t)$ is singular for $p_4(t) \equiv 0$ in a subinterval of $[0, T]$. (29)

In a singular subarc, the corresponding control variable is not necessarily bang-bang and has to be determined by exploiting the vanishing of its switching function. The details of the analysis are deleted. Using the optimal control laws (28) and (29), solving the two-point-boundary-value problem for each pair of initial and final states, and verifying that a globally time-optimal control has been found, leads to the complete optimal solution which is summarized in the following subsection.

D. The Time-Optimal Solution

1) The Regular Time-Optimal Solution: The regular time-optimal control is purely bang-bang for both of the control variables. The nature of the optimal solution is most conspicuous in the special case where the initial radius r_a (15) and the final radius r_b (18) are identical, i.e., when a simple motion in azimuth is requested. In Fig. 2, the optimal position trajectories $x_1(t) = r(t)$ and $x_3(t) = \varphi(t)$ and the optimal costate trajectories $p_2(t)$ and $p_4(t)$ determining the optimal controls are shown for $r_a = r_b = 0.15$ m, $\varphi_a = 0$, and $\varphi_b = \pi/2$ rad. The azimuth coordinate is slewed in the obvious bang-bang fashion. However, in addition, the radial coordinate performs a nontrivial bang-bang pull-in/push-out movement. The physical interpretation of the optimal motion is quite simple. By pulling in the hand and the load and then pushing it out again using maximal (absolute) force at all times, the mass moment of inertia of the robot with respect to the azimuth axis is minimized, and hence the angular acceleration/deceleration maximized at all times $t \in [0, T]$. The optimal force switches twice, $u_1: \{-F_{\max}, +F_{\max}, -F_{\max}\}$; the optimal torque switches once, $u_2: \{+M_{\max}, -M_{\max}\}$. In this numerical example, the optimal final time of 1.16 s is 20 percent below the transfer time of 1.46 s for a bang-bang torque with the radius r held constant.

2) Time-Optimal Solutions with Singular Arcs: If the angle $\varphi_b - \varphi_a$ is large (>0) and the maximal force $F_{\max}$ is sufficiently high, then the center of gravity of the complete arm (naked arm, hand, and load) could cross the azimuth axis if a purely bang-bang force was used. Continuing the translatory movement would result in an increase of the mass moment of inertia rather than a further decrease. Then the following singular arc is optimal:

$$u_1(t) = F(t) \equiv 0 \text{ with} \tag{30}$$

$$x_1(t) = r(t) \equiv -m_n r_0/(m_a + m_n). \tag{31}$$

The angular movement continues to be bang-bang. Notice that the centers of gravity S of the naked arm and of the hand are on opposite sides of the azimuth axis. Thus, the optimal force switches four times, $u_1: \{-F_{\max}, +F_{\max}, 0, +F_{\max}, -F_{\max}\}$; the optimal torque switches once, $u_2: \{+M_{\max}, -M_{\max}\}$.

If the angle $|\varphi_b - \varphi_a|$ is small and $|r_b - r_a|$ is large, then the optimal motion contains a singular arc with

$$u_2(t) = M(t) \equiv 0 \text{ with} \tag{32}$$

$$x_3(t) = \varphi(t) \equiv \text{constant}. \tag{33}$$

For $r_b > r_a$ and $\varphi_b > \varphi_a$ the time-optimal trajectory is regular in the beginning and singular towards the end. The optimal force switches once, $u_1: \{+F_{\max}, -F_{\max}\}$; the optimal torque switches three times, $u_2: \{+M_{\max}, -M_{\max}, +M_{\max}, 0\}$. The azimuth angle $\varphi(t)$ overshoots beyond the final angle φ_b during the trajectory. The physical explanation is as follows. In the initial phase, the translatory acceleration of the arm is enhanced by the centrifugal force and, therefore, both the maximal force $+F_{\max}$ and the maximal torque $+M_{\max}$ are applied. In the second phase the required azimuth maneuver is terminated. In the final phase the robot's azimuth is identical to the final azimuth φ_b. The centrifugal force vanishes. Therefore, the final translatory deceleration to stand still is maximal.

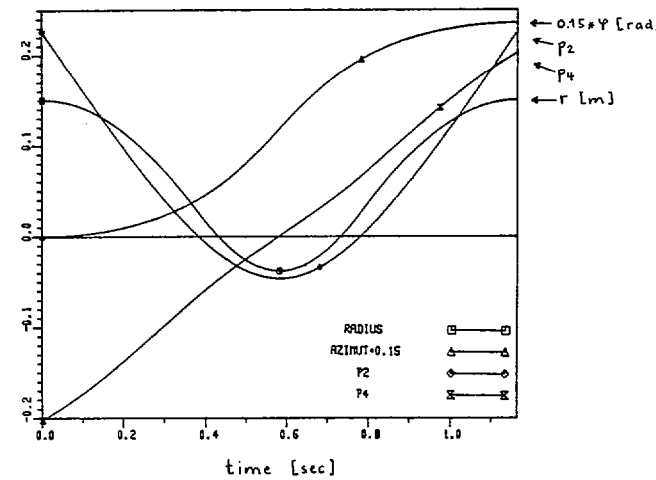

Fig. 2. Regular time-optimal motion of the cylindrical robot.

For $r_b < r_a$ and $\varphi_b > \varphi_a$ the time-optimal trajectory is singular in the beginning and regular towards the end. The optimal switching sequences are $u_1: \{-F_{\max}, +F_{\max}\}$ and $u_2: \{0, -M_{\max}, +M_{\max}, -M_{\max}\}$. Finally, for $\varphi_b - \varphi_a < 0$ the trajectories which are symmetric to the above ones obtained.

III. Robots with Spherical Coordinates

In this section, two spherical robots are discussed. The geometry of the first is shown in Fig. 3. The first degree of freedom is the angular azimuth position α. The second degree of freedom is the angular elevation position λ. This configuration corresponds to an anti-aircraft gun mount.

With the state variables

$$x_1(t) = \lambda(t) \tag{34}$$

$$x_2(t) = \dot{\lambda}(t) \tag{35}$$

$$x_3(t) = \alpha(t) \tag{36}$$

$$x_4(t) = \dot{\alpha}(t) \tag{37}$$

and with the two controlled torques

$$u_1(t) = M_\lambda(t) \tag{38}$$

$$u_2(t) = M_\alpha(t) \tag{39}$$

and neglecting friction and the influence of gravity (which is assumed to be compensated for by suitable means) the equations of motion can be written as follows:

$$\dot{x}_1(t) = x_2(t) \tag{40}$$

$$\dot{x}_2(t) = [u_1(t) + (\theta_x - \theta_z)\sin(x_1(t))\cos(x_1(t))x_4^2(t)]/\theta_y \tag{41}$$

$$\dot{x}_3(t) = x_4(t) \tag{42}$$

$$\dot{x}_4(t) = [u_2(t) - 2(\theta_x - \theta_z)\sin(x_1(t)) \cdot \cos(x_1(t))x_2(t)x_4(t)]/\theta(x_1(t)) \tag{43}$$

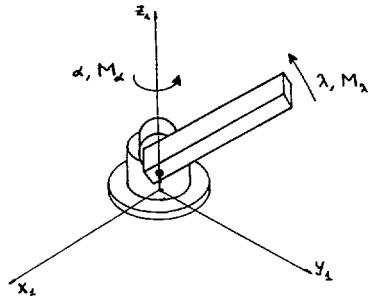

Fig. 3. Sketch of the 2 d.o.f. spherical robot.

where

θ_x = mass moment of inertia of the arm, the hand, and the load w.r. to the axis of the arm (44)

θ_y = mass moment of inertia of the arm, the hand, and the load w.r. to the elevation axis (45)

θ_z = mass moment of inertia of the robot w.r. to the azimuth axis for $\lambda = 0$ (46)

$$\theta(x_1(t)) = \theta_x \sin^2(x_1(t)) + \theta_z \cos^2(x_1(t)). \tag{47}$$

The control constraints are

$$|u_1(t)| \leq M_{\lambda,\max} \tag{48}$$

$$|u_2(t)| \leq M_{\alpha,\max}. \tag{49}$$

The analysis of time-optimal motions of this robot proceeds in a way which is completely analogous to that of Section II-C.

The regular time-optimal motion is bang-bang in both of the controls. The nature of this solution is most conspicuous in the special case where the requested transfer is a pure change of azimuth (i.e., $\lambda_b = \lambda_a$). The bang-bang movement in elevation (towards the zenith) serves to minimize the azimuthal mass moment of inertia at all times $t \in [0, T]$.

If the requested azimuth transfer is small and the elevation transfer is towards the zenith (i.e., $\lambda_b > \lambda_a \geq 0$), then the time-optimal solution has an initial singular arc with $u_2(t) = M_\alpha(t) \equiv 0$ followed by a regular arc. The character of this trajectory is again explained by the centrifugal force.

The third degree of freedom of the second type of spherical robots is the translatory, radial position of the arm. The time-optimal motions of this robot should now be fairly obvious. In the regular case both of the torques and the radial force are bang-bang. The "extra" angular movement in elevation and translatory movement of the arm serve to minimize the azimuthal mass moment of inertia at all times. Again, there are time-optimal motions containing singular arcs.

IV. Robot with an Articulated Arm

A. The Model

The geometry of the robot with a horizontal arm consisting of two links is shown in Fig. 4. For numerical studies, approximate data for the IBM 7535 B 04 robot are used. The first degree of freedom is the vertical translation z. This coordinate is not treated here because it is completely decoupled both from the second and the third coordinate. The second degree of freedom is the angular rotation φ of the inner link. The third degree of freedom is the (relative) angular rotation ψ of the outer link. Both of the coordinates are driven by limited torques M_φ and M_ψ, respectively. The remaining degrees of freedom used for positioning the end effector are neglected.

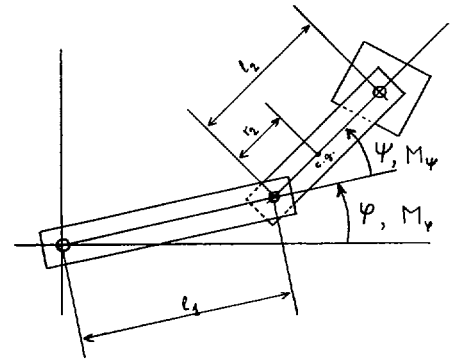

Fig. 4. Sketch of the IBM 7535 B 04 robot.

With the state variables

$$x_1(t) = \varphi(t) \tag{50}$$

$$x_2(t) = \dot{\varphi}(t) \tag{51}$$

$$x_3(t) = \psi(t) \tag{52}$$

$$x_4(t) = \dot{\psi}(t) \tag{53}$$

and the control variables

$$u_1(t) = M_\varphi(t) \tag{54}$$

$$u_2(t) = M_\psi(t) \tag{55}$$

and neglecting friction (and dropping the notation for dependence on time t) the equations of motion are

$$\dot{x}_1 = x_2 \tag{56}$$

$$\dot{x}_2 = [\theta_7\{u_1 - u_2 + \theta_6(x_2 + x_4)^2 \sin(x_3)\} - \theta_6 \cdot \{u_2 - \theta_6 x_2^2 \sin(x_3)\} \cos(x_3)]/[\theta_7\theta_5 - \theta_6^2 \cos^2(x_3)] \tag{57}$$

$$\dot{x}_3 = x_4 \tag{58}$$

$$\dot{x}_4 = [(\theta_5 + \theta_6 \cos(x_3))\{u_2 - \theta_6 x_2^2 \sin(x_3)\} - (\theta_7 + \theta_6 \cos(x_3)) \cdot \{u_1 - u_2 + \theta_6(x_2 + x_4)^2 \sin(x_3)\}]/[\theta_7\theta_5 - \theta_6^2 \cos^2(x_3)] \tag{59}$$

where

θ_1 = mass moment of inertia of the link 1 w.r. to the first axis

θ_2 = mass moment of inertia of the link 2 w.r. to the second axis

θ_3 = mass moment of inertia of the hand and the load w.r. to the position of the hand

$$\theta_4 = \theta_2 + l_2^2 m_3$$

$$\theta_5 = \theta_1 + l_1^2(m_2 + m_3)$$

$$\theta_6 = l_1(r_2 m_2 + l_2 m_3)$$

$$\theta_7 = \theta_3 + \theta_4$$

m_2 = mass of the second link

m_3 = mass of the hand and the load

l_1, l_2 = lengths of the links 1 and 2, respectively,

r_2 = distance between the center of gravity of the second link and its driving axis. (60)

The control constraints are

$$|u_1(t)| \le M_{\varphi,\max} \tag{61}$$

$$|u_2(t)| \le M_{\psi,\max}. \tag{62}$$

For the numerical calculations the following values were used for the IBM 7535 B 04 robot:

$$\theta_1 = 1.6 \text{ m}^2\text{kg} \quad \theta_2 = 0.43 \text{ m}^2\text{kg} \quad \theta_3 = 0.01 \text{ m}^2\text{kg}$$

$$l_1 = 0.4 \text{ m} \quad l_2 = 0.25 \text{ m} \quad r_2 = 0.125 \text{ m}$$

$$m_2 = 15 \text{ kg} \quad m_3 = 6 \text{ kg}$$

$$M_{\varphi,\max} = 25 \text{ Nm} \quad M_{\psi,\max} = 9 \text{ Nm}. \tag{63}$$

B. Analysis of the Time-Optimal Control Problem

Mathematically, the analysis proceeds along the lines of Section II-C. The Hamiltonian again is affine in the controls u_1 and u_2. Hence, the controls are bang-bang or may be singular if the switching functions (multiplying u_1 and u_2, respectively) are nonzero or identically zero over some interval, respectively.

From the physical side, the experience with the cylindrical and the spherical robots suggests that the outer link should be folded inward in order to reduce the mass moment of inertia seen by M_φ. However, a new phenomenon is relevant as well. The torque M_ψ both acts onto the outer link and reacts onto the inner link. Hence, the torque M_ψ increases (decreases) the accelerating effect of the torque M_φ if the two torques have opposite (equal) signs. Therefore, the torques can be expected to have opposite signs at the beginning and at the end of the motion in many cases.

The results of the detailed numerical analysis can be summarized as follows.

C. The Time-Optimal Solution

The structure of the time-optimal solution will mainly be discussed for the special case where the robot's arm is stretched both in the initial and in the final position, i.e., for the boundary conditions

$$x_1(0) = \varphi_a = 0 \tag{64}$$

$$x_3(0) = \psi_a = 0 \tag{65}$$

$$x_1(T) = \varphi_b > 0 \tag{66}$$

$$x_3(T) = \psi_b = 0, \text{ or } \pm 2\pi, \text{ or } \cdots \tag{67}$$

$$x_2(0) = x_4(0) = x_2(T) = x_4(T) = 0. \tag{68}$$

Obviously, for $\varphi_b < 0$ the solution is symmetric. Furthermore, the interesting region of motion is $0 \le \varphi_b \le \pi$. Since the set of admissible final states is not convex, the individual values for ψ_b in (67) will be investigated separately. The overall globally time-optimal solution will be chosen among these solutions by comparing the transfer times for each value of the angle φ_b.

For a positive final angle φ_b of the inner arm, for the outer arm not swinging through, i.e., $\psi_b = 0$, and for the numerical values of (63) the types of time-optimal solutions summarized in Table I are obtained.

For $\varphi_b = 0 \cdots 0.98$, the solution is regular and its type is designated A_0. The optimal torque M_φ switches once, $u_1: \{+M_{\varphi,\max}, -M_{\varphi,\max}\}$; the optimal torque M_ψ switches twice, $u_2: \{-M_{\psi,\max}, +M_{\psi,\max}, -M_{\psi,\max}\}$. (In Table I, this characterization is further abridged to $\{+, -\}$ and $\{-, +, -\}$, respectively.) A stroboscopic picture of the optimal motion of type A_0 is shown in Fig. 5. (The strobing is at equidistant times. The switching times of the torques are indicated in the figure captions.)

TABLE I
IBM 7535 B 04 ROBOT: TYPES OF TIME-OPTIMAL SOLUTIONS WITHOUT SWINGING THROUGH (i.e., $\psi_b = 0$)

angle φ_b [rad]	type of solution	switching sequences for $u_1 = M_\varphi$	for $u_2 = M_\psi$
$0 \cdots 0.98$	A_0	$\{+, -\}$	$\{-, +, -\}$
$0.98 \cdots \pi$	A_1	$\{+, -, +\}$	$\{-, +, -\}$

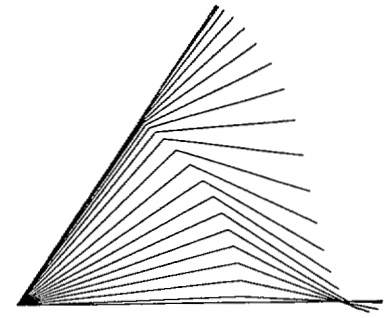

Fig. 5. Time-optimal motion of type A_0: switching time for $u_1 = M_\varphi$: 0.5425 s; switching times for $u_2 = M_\psi$: 0.088 and 0.588 s; final time: $T = 1.085$ s.

For $\varphi_b = 0.98 \cdots \pi$ the solution is regular, too, and its type is designated A_1. The optimal torque M_φ switches twice, $u_1: \{+M_{\varphi,\max}, -M_{\varphi,\max}, +M_{\varphi,\max}\}$; the optimal torque M_ψ also switches twice, $u_2: \{-M_{\psi,\max}, +M_{\psi,\max}, -M_{\psi,\max}\}$. An example of an optimal motion of type A_1 is displayed in Fig. 6. In both of the examples of Figs. 5 and 6, the final positions φ_b of the robot are very close to the boundary separating the sectors A_0 and A_1. Notice that the motion in Fig. 6 (type A_1) has a short interval each at the start and at the end of $[0, T]$ where the two torques have opposite signs. Hence, both the starting acceleration and the stopping deceleration of the inner arm are maximal. The type A_0 is the only one which does not allow such intervals at *both* ends because the angle of transfer φ_b is too small.

For very high values of φ_b the solution would contain a singular arc in the middle (type A_2). For the characteristics of the singular arc the reader is referred to the discussion of the singular arc of the type B_2 below. Irrespective of the numerical values of (63) the transfer time for the type A_2 would be longer than for the type B_2. Therefore, the type A_2 is not discussed in detail here. ($u_1: \{+M_{\varphi,\max}, -M_{\varphi,\max}, +M_{\varphi,\max}\}$; $u_2: \{-M_{\psi,\max}, +M_{\psi,\max}, -M_{\psi,\text{sing}}, +M_{\psi,\text{sing}}, +M_{\psi,\max}, -M_{\psi,\max}\}$; φ overshooting φ_b as in A_1.)

For a positive final angle φ_b of the inner arm, for the outer arm swinging through to $\psi_b = -2\pi$, and for the numerical values of (63) the types of time-optimal solutions summarized in Table II are obtained.

For $\varphi_b = 0 \cdots 1.76$ the solution is regular and its type is designated B_0. The optimal torque M_φ switches three times, $u_1: \{+M_{\varphi,\max}, -M_{\varphi,\max}, +M_{\varphi,\max}, -M_{\varphi,\max}\}$; the optimal torque M_ψ switches once at $t = T/2$, $u_2: \{-M_{\psi,\max}, +M_{\psi,\max}\}$. A stroboscopic picture of the optimal motion of type B_0 is shown in Fig. 7.

For $\varphi_b = 1.76 \cdots 3.51$ the solution again is regular and its type is designated B_1. The optimal torque M_φ switches once at $t = T/2$, $u_1: \{+M_{\varphi,\max}, -M_{\varphi,\max}\}$; the optimal torque M_ψ switches three times, $u_2: \{-M_{\psi,\max}, +M_{\psi,\max}, -M_{\psi,\max}, +M_{\psi,\max}\}$. An example of an optimal motion of type B_1 for $\varphi_b = \pi$ is displayed in Fig. 8.

For $\varphi_b > 3.51$ the solution contains a singular arc in the middle and its type is designated B_2. The singular arc is characterized by the outer arm being held folded at $\psi \equiv -\pi$. For the folded outer arm the mass moment of inertia w.r. to the first axis is minimal.

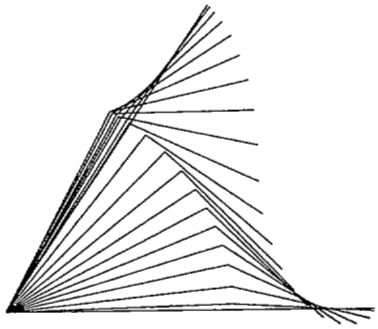

Fig. 6. Time-optimal motion of type A_1: switching times for $u_1 = M_\varphi$: 0.513 and 1.056 s; switching times for $u_2 = M_\psi$: 0.113 and 0.634 s; final time: $T = 1.085$ s.

TABLE II
IBM 7535 B 04 ROBOT: TYPES OF TIME-OPTIMAL SOLUTIONS WITH SWINGING THROUGH (i.e., $\psi_b = -2\pi$)

angle φ_b [rad]	type of solution	switching sequences for $u_1 = M_\varphi$	for $u_2 = M_\psi$
$0 \cdots 1.76$	B_0	$\{+, -, +, -\}$	$\{-, +\}$
$1.76 \cdots 3.51$	B_1	$\{+, -\}$	$\{-, +, -, +\}$
>3.51	B_2	$\{+, -\}$	$\{-, +, -\text{sing.}, +\text{sing.}, -, +\}$

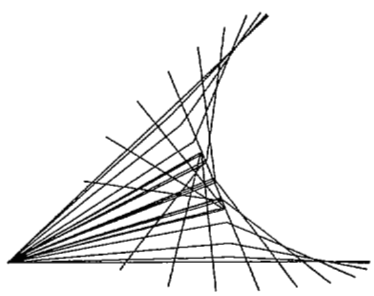

Fig. 7. Time-optimal motion of type B_0: switching times for $u_1 = M_\varphi$: 0.190, $T/2$, and 0.785 s; switching time for $u_2 = M_\psi$: $T/2$; final time: $T = 0.9755$ s.

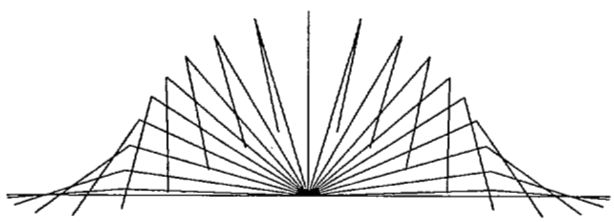

Fig. 8. Time-optimal motion of type B_1: switching time for $u_1 = M_\varphi$: $T/2$; switching times for $u_2 = M_\psi$: 0.278, $T/2$, and 0.974 s; final time: $T = 1.252$ s.

While the first axis applies maximal torque the singular clamping torque for the second axis is given by

$$M_{\psi,\text{sing}}/M_{\varphi,\max} = (\theta_7 - \theta_6)/(\theta_5 - 2\theta_6 + \theta_7) = -0.174. \quad (69)$$

For the numerical example of (63) the singular torque is admissible. The optimal torque M_φ switches once (at $t = T/2$), $u_1: \{+M_{\varphi,\max}, -M_{\varphi,\max}\}$; the optimal torque M_ψ switches five times, $u_2: \{-M_{\psi,\max}, +M_{\psi,\max}, -M_{\psi,\text{sing}}, +M_{\psi,\text{sing}}, -M_{\psi,\max}, +M_{\psi,\max}\}$. The solution is completely symmetrical w.r. to $t = T/2$. However, the type B_2 is not relevant in this case because $3.51 > \pi$.

At the boundary of the regions B_0 and B_1 both of the optimal torques switch once at $t = T/2$, $u_1: \{+M_{\varphi,\max}, -M_{\varphi,\max}\}$, $u_2: \{-M_{\psi,\max}, +M_{\psi,\max}\}$, i.e., the two central intervals of the switching sequences of M_φ and M_ψ, respectively, collapse. In the case of the type B_0, the inner torque M_φ is "too strong" and has to kill time in the central phase with a bang-bang correcting maneuver for M_φ. The reaction force in the outer joint resulting from the correcting torque M_φ increases the accelerating/decelerating effect of the torque M_ψ on the outer arm. In the case of the type B_1, the outer torque M_ψ is "too strong" and has to kill time in the central phase with a bang-bang correcting maneuver for M_ψ. For B_1 the bang-bang correcting maneuver can be viewed as an effort to keep the arm more or less folded for an extended period around $t = T/2$. Notice, however, that the angular velocity $d\psi/dt$ of the outer arm always is strictly negative throughout the trajectory. At the boundary of the regions B_1 and B_2 $d\psi/dt$ vanishes at $T/2$ and in the sector B_2 $d\psi/dt$ vanishes throughout the singular arc.

Comparing the solutions of types A and B w.r. to the resulting transfer times for all $0 \le \varphi_b \le \pi$, the overall globally time-optimal solution is found as summarized in the Table III. Notice that in this numerical example the types A_1 and B_2 happen to disappear.

For the numerical values of (63) a comparision of the optimal transfer time T_{opt} with suboptimal ones is given in Table IV. The column T_n refers to the motion of the stiff straight arm using the obvious bang-bang control for M_φ. The column T_A applies to the suboptimal solutions of the type A_1.

Remark 1: It should be noted that all of the time-optimal motions have equivalent symmetric partners. These are obtained from the above solutions by reversing the control variables with respect to time and by inverting their sign. The stroboscopic pictures of their motions are symmetric to the above ones with respect to the corresponding radial line at $\varphi_b/2$. This may be important to know when position constraints have to be taken into account.

Remark 2: For the more general case where the initial and/or the final position of the robot's arm does not correspond to a straight arm analogous calculations of optimization can be carried out. The physical phenomena responsible for the nature of the time-optimal solutions remain the same as above. Therefore, the possible types of optimal solutions are expected to be the same. For some ranges of the initial and final angles φ_a, ψ_a, and φ_b, ψ_b, respectively, and depending on the numerical values (63) some of the types A_0, A_1, A_2, B_0, B_1, and B_2 of solutions may disappear again.

V. Computational Remarks

For the numerical analysis of the examples in Section IV both a shooting algorithm for solving the two-point-boundary-value problems and a parameter optimization method were used. The authors were unable to find any solution for the IBM robot using the shooting method *only*.

Therefore, the parameter optimization was utilized in order to find the switching times for the controls, starting with various control parametrizations, minimizing the problem duration, and using the penalty approach for the prescribed final state. With a shooting algorithm for solving two-point-boundary-value problems it was verified that the solution satisfied *all* of the necessary conditions of Pontryagin's minimum principle. Convergence of the shooting algorithm was achieved with the Lagrange multiplier of the penalty term of the previous step as an initial guess for the final costate vector.

VI. Conclusions

In this paper, the *structure* of the time-optimal motions of a robot with cylindrical coordinates has been given. For a robot with a horizontal articulated arm with two links the *structure* of

TABLE III
IBM 7535 B 04 ROBOT: GLOBALLY TIME-OPTIMAL SOLUTION FOR $0 \leq \varphi_b \leq \pi$

angle φ_b [rad]	type of solution	switching sequences for $u_1 = M_\varphi$	for $u_2 = M_\psi$
$0 \cdots 0.76$	A_0	$\{+, -\}$	$\{-, +, -\}$
$0.76 \cdots 1.76$	B_0	$\{+, -, +, -\}$	$\{-, +\}$
$1.76 \cdots \pi$	B_1	$\{+, -\}$	$\{-, +, -, +\}$

TABLE IV
COMPARISON OF TRANSFER TIMES FOR THE IBM 7535 B 04 ROBOT

angle φ_b [rad]	type	time-optimal T_{opt} [sec]	stiff arm T_n [sec]	suboptimal, type A_1 T_A [sec]
π	B_1	1.25	2.06	1.51
1.76	$B_0 = B_1$	0.92	1.54	1.27
$\pi/2$	B_0	0.92	1.46	1.24
0.76	$A_0 = B_0$	0.98	1.02	

the time-optimal motions has been given for the special case where the robot's arm is straight both initially and finally. The case of the spherical robot with two and three degrees of freedom has also been discussed. The most important *physical effects* responsible for the nature of the time-optimal solutions have been revealed: 1) minimization of the mass moment of inertia with respect to revolute joints; 2) enhancement of accelerations/decelerations by exploiting reaction torques and forces. It has been demonstrated that the savings in transfer times are considerable in comparision with simpler trajectories (chosen in some pragmatic or more natural way).

The philosophy of this paper is that the structure of the time-optimal motion of a new robot in the absence of state constraints but in the presence of the control constraints should be known when the robot is in its (mechanical) design phase. This knowledge allows us to fix the design parameters (control constraints, masses, inertias, state constraints) in a way leading to maximal productivity of the robot.

The IBM 7535 B 04 robot does not allow all of the motions proposed in Section IV in both directions because it has a mechanical stop for ψ for the straight position of the arm and because it does not allow the outer arm to swing through. Obviously, much could be gained by the absence of these position constraints. The steps to be undertaken in a redesign would be fairly straightforward.

In this paper, the resulting time-optimal solutions are in open-loop form, i.e., the optimal controls are known as functions of time only rather than as functions of the instantaneous state vector. The conversion of the optimal open-loop solutions to their closed-loop form is theoretically feasible. In practice, this is the most difficult step and is very much an open problem of research. The problem is further increased by the need for incorporating into the closed-loop control scheme the unavoidable state constraints of the real robot.

REFERENCES

[1] M. E. Kahn, "The near minimum-time control of open-loop articulated kinematic chains," Ph.D. dissertation, Stanford Univ., Stanford, CA, Dec. 1969, Microfiche Nr. AD 708 076.

[2] G. N. Saridis and C. S. G. Lee, "Approximation theory of optimal control for trainable manipulators," *IEEE Trans. Syst. Man Cybern.*, vol. SMC-9, pp. 152-159, 1979.

[3] T. L. Turner and W. A. Gruver, "Viable suboptimal controller for robotic manipulators," in *Proc. 19th IEEE Conf. on Decision Contr.*, Albuquerque, NM, Dec. 1980, pp. 83-87.

[4] R. Gawronski, I. Pardyka, A. Pawlowski, and W. Wolski, "Time-optimal hierarchical control system of manipulator movement with adaptive on-off control," *Syst. Sci.*, vol. 7, pp. 167-177, 1981.

[5] L. K. Huang, "Control of a tendon arm," Artificial Intelligence Lab., Mass. Inst. Technol., Rep. AI-M-617, Feb. 1981.

[6] T. L. Johnson, "On feedback laws for robotic systems," Mass. Inst. Technol., Lab. Inform. Sci. and Syst., Cambridge, MA, Rep. AFOSR-TR-81-0456, Apr. 1981.

[7] N. N. Bolotnik and A. A. Kaplunov, "Optimal rectilinear moving a load with a two-link manipulator," *Eng. Cybern.*, vol. 20, pp. 121-131, 1982.

[8] M. Vukobratovic and M. Kircanski, "Method for optimal synthesis of manipulation robot trajectories," *J. Dynam. Syst. Meas. Contr.*, vol. 104, pp. 188-193, 1982.

[9] P. Marinov and P. Kiriazow, "A direct method for optimal control synthesis of manipulator point-to-point motion," in *Proc. 9th IFAC World Congress*, Budapest, Hungary, Aug. 1984, paper 14.2/G-5.

[10] K. G. Shin and N. D. McKay, "Robot path planning using dynamic programming," in *Proc. 23rd Conf. Decision Contr.*, Las Vegas, NV, Dec. 1984, pp. 1629-1635.

[11] F. Pfeiffer, "On optimal control of manipulator trajectories," *J. Dynam. Syst. Contr.*, submitted for publication.

[12] M. Athans and P. L. Falb, *Optimal Control*, New York: MacGraw-Hill, 1966.

[13] J. E. Bobrow, S. Dubowsky, and J. S. Gibson, "On the optimal control of robotic manipulators with actuator constraints," in *Proc. 1983 Amer. Contr. Conf.*, San Francisco, CA, June 1983, pp. 782-787.

Hans P. Geering (S'70-M'71-SM'78) was born on June 7, 1942. He received the Dipl. El.-Ing. ETH degree from the Swiss Federal Institute of Technology (ETH), Zurich, Switzerland, in 1966, and the M.S. and Ph.D. degrees from the Massachusetts Institute of Technology, Cambridge, in 1969 and 1971, respectively.

From 1967 to 1968 and from 1971 to 1979 he was with the Military Products Division of Oerlikon-Buehrle AG, Zurich. From 1968 to 1971 he was a Research Assistant at the M.I.T. Electronic Systems Laboratory. He joined the faculty of the Department of Mechanical Engineering, ETH, Zurich, in 1979, where he is currently a Professor of Measurement and Control. His research interests are in optimal control and estimation and in automotive and robot control.

Dr. Geering is a member of the American Institute of Aeronautics and Astronautics, the American Society of Mechanical Engineers, the Society of Automotive Engineers, and the Swiss societies SEV and SGA (IFAC).

Lino Guzzella was born on October 13, 1957. He received the Dipl. Masch.-Ing. ETH degree from the Swiss Federal Institute of Technology (ETH), Zurich, Switzerland, in 1981.

At present he is a Research Assistant in the Measurement and Control Laboratory of ETH, Zurich, where he is completing his Ph.D. thesis on variable structure control systems. His research interests include optimal control and the implementation of digital controllers with microprocessors and/or custom-VLSI chips.

Stephan A. R. Hepner was born on December 26, 1955. He received the Dipl. Masch.-Ing. ETH degree from the Swiss Federal Institute of Technology (ETH), Zurich, Switzerland, in 1982.

At present he is a Research Assistant in the Measurement and Control Laboratory of ETH, Zurich, where he is completing his Ph.D. thesis in the area of AA missile guidance. His research interests are in algorithms for solving optimization problems, nonlinear filtering theory, and applications of the singular perturbation theory.

Mr. Hepner is a member of the American Institute of Aeronautics and Astronautics and SGA.

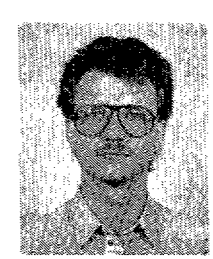

Christopher H. Onder was born on November 14, 1961. He received the Dipl. Masch.-Ing. ETH degree (with honors) from the Swiss Federal Institute of Technology (ETH), Zurich, Switzerland, in 1984.

At present he is a Research Assistant in the Measurement and Control Laboratory of ETH, Zurich, where he is working on optimal control of automotive engines. His research interests are in optimal control and estimation.